On Growth Patterns of Branched Polymer Architectures

Piet D. Iedema, Huub C.J. Hoefsloot*

Universiteit van Amsterdam, Dept. Chem. Eng., Nieuwe Achtergracht 166, 1018 WV Amsterdam, Netherlands
E-mail: piet@science.uva.nl.

Summary: In nature trees may have many different forms and so have all natural branched structures. Differences in branched architectures of synthetic polymers can only be explained by kinetics. We compare radical polymerization of low density Polyethylene (PE) and PE polymerization with Constrained Geometry Catalyst (CGC) metallocene. The architectures generated by our synthesis algorithms revealed marked differences between the two PE-systems. Metallocene-PE turned out to be more comb-like. This could partially be explained by analyzing growth patterns of the two PE types as incorporated in the architecture synthesis algorithms.

Keywords: branched; Monte Carlo simulation; polyethylene; rheology; topology

Introduction

A fascinating rheology is what have most branched polymers in common. Recently, this has been explained in terms of molecular topology, the connectivity between branch points.[1,2] In earlier work, we have attempted to explain topology from kinetics for radical polymerization of ldPE[3] and CGC-metallocene catalyzed PE.[2] The present paper focuses on the similarities and differences of the two systems.

In both cases we identified linear segments as the basic constituting elements of the structures. The length distribution and the coupling mechanics of these elements are characterized by a start mechanism, a growth and a termination. These factors determine the topology. In ldPE the branch forming mechanism is transfer to polymer. On an existing chain a new growth center is formed, from which grows a long side branch. The linear segment here is identified as 'primary polymer (pp)'. Growth start happens either by new initiation or by formation of a secondary radical position along an already existing chain. Pp length is determined by the competition between propagation and a termination mechanism. A characteristic of this system is that coupling of pps may happen at *any position* of the pp. Typically, pp length distribution obeys Flory. In the metallocene case branches are formed by insertion of already formed chains with an unsaturated chain (terminal double bond, TDB) end into growing polymer. The linear elements here are the segments between branch points and free arms, connected to the molecule at one end only. Start

 DOI: 10.1002/masy.200450208

of segment growth is either by initiation of a new chain or by insertion of a TDB ended chain. In the one-catalyst system considered here the length expectation of all these segments is the same; it obeys a Flory distribution. The main difference with the ldPE system is the coupling mechanism, since coupling is only at *end* points. Another highly important factor in the ldPE case is chain scission, of which the kinetics in itself depends on topology.

For both systems we have developed algorithms based on *conditional* Monte Carlo sampling to predict architectures, meaning that sampling happens at given chain length, n, and number of branch points, N. The bivariate chain length/number of branch points concentration distribution (CLD/NBD) is typically calculated by solving population balances using a Galerkin-finite element model (G-FEM) using the software package PREDICI®.[4-6] The conditional MC method is computationally more efficient than the full MC method since it directly focuses on the chains with many branch points.

In this paper we start with a brief description of the kinetics of both systems. Then a more detailed description follows of the architectures synthesizing algorithms. Results are presented in terms of radius of gyration and rheological qualifiers of branched molecules.

Kinetics

Regarding ldPE, apart from the usual initiation, propagation, termination and transfer mechanisms, following mechanisms are essential for the branching topology:[4]

Transfer to polymer: $R_{n,i} + P_{m,j} \xrightarrow{k_{tp}m} P_{n,i} + R_{m,j+1}$

Chain scission by hydrogen abstraction: $R_{n,i} + P_{m,j} \xrightarrow{k_{ts}m} P_{n,i} + R_{m-r,j-k} + P_{r,k}$

Here, R and P denote living and dead polymer, resp., while subscripts refer to chain length and number of branches. Note in the case of scission that fragment lengths m-r and r are preferentially short and long, due to typical scission characteristics of branched structures.[3] These characteristics could be obtained by exploring the fragment length distributions resulting from randomly breaking architectures synthesized by the algorithm to be discussed next.

In the CGC-system the mechanisms responsible for branch formation are β-hydride elimination, yielding macromonomers with unsaturated chain ends, and incorporation of macromonomers at catalyst-sites:[2,6-8]

β-hydride elimination: $R_n \xrightarrow{k_{\beta H}} C^*_{CGC} + P^=_n$

TDB-propagation: $R_n + P^=_m \xrightarrow{k_{p,TDB}} R_{n+m}$

Kinetic coefficients are listed elsewhere.[2,6] Population balances have been solved using the G-FEM model, yielding CLD/NBD as depicted in Figure 1.[6] Since the G-FEM model solves the branching distribution balances as moment equations (pseudo-distribution approach[4,5]), an assumption has to be made as to the shape of the branching distribution at given chain length, n. In the case of ldPE the CLD is governed by the combinatorics of Flory distributed *primary*

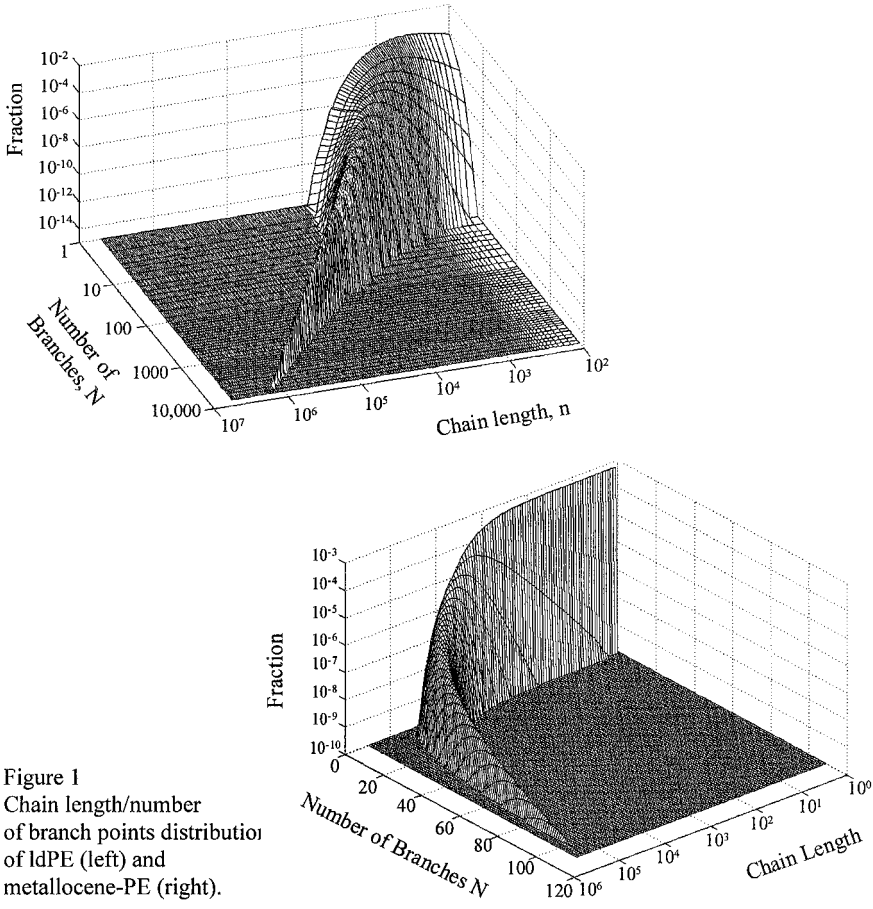

Figure 1
Chain length/number of branch points distributio of ldPE (left) and metallocene-PE (right).

polymers, linear elements carrying branch points.[3] This leads to a binomial distribution (BD) of branches at given n. In contrast, metallocene-PE combinatorics are determined by Flory distributed *segments,* either between adjacent branch points or free arms. This leads to a branching distribution that is *narrower* than a BD. To this end we had to use a variable power BD (VPBD) approximation in combination with the second branching moment from G-FEM pseudo-distribution model yielding almost perfect agreement with the rigorous solution.[6]

Architectures synthesis

ldPE. The synthesis algorithm is based on the primary polymers (pps) as the basic linear elements (Figure 2). A molecule with N branch points is composed of N+1 pps. Pp growth starts at either new chain initiation or at a secondary radical along an already existing chain after a transfer to polymer reaction. Pp length is determined by the competition between propagation on one hand and termination, transfer to small molecules and scission on the other. Pp lengths are Flory distributed and are simply calculated from kinetics.[3]

The first step of the algorithm is sampling N+1 pps from the calculated distribution. This is realized as follows. We pick N numbers at random between 0 and n and arranging them in ascending order. Together with 0 at the beginning and n at the end this gives a series of N+2 numbers. Series containing two or more equal numbers are discarded. The N+1 differences between successive numbers are the pp lengths; they are Flory distributed. The next step is finding the growth time sequence of pps in the molecule to be composed. This determines which pp may have grown from which other already existing pp. Notice that pp growth may be regarded instantaneous in this radical system.

The connection part of the algorithm is simple after the time order has been determined; see Figure 2. The 2^{nd} pp selected is attached to pp 1; the 3^{rd} may be attached to pps 1 and 2; etc. The algorithm accounts for the fact that the pp's probability of receiving a branch point is proportional to its length, which reflects branch formation by transfer to polymer. Furthermore, it accounts for the pp's differences in residence time. A pp early in time order – meaning a pp with a long residence time – has a higher chance of receiving branch points than a later pp. It implies that branch point distribution is *heterogeneous*, since pps with a longer residence time possess a higher branching density.

Metallocene-PE. In the case of a single catalyst the method is based on the separation of the synthesis activities concerning topology and segment lengths. This is allowed, since all chain segments in a molecule of given n and N should obey the same statistics, since all of them grown under the same kinetic conditions.[1,9] This fact implies that interchanging any pair of segments does not affect the probability of existence of a structure as long as it retains the same topology. This implies that we can determine first the topology and afterwards the length of the segments.

As a first step of the topology synthesis procedure we consider the first insertion of a terminal double bonded polymer structure into a growing chain attached to the branching catalyst. The number of branch points on the inserted chain, N_1, and the number of branch points on the growing chain (to be formed after the first insertion) must add up to N-1. The situation is depicted in Figure 2. Note that with a single catalyst, at steady-state in a CSTR, the statistical properties of the inserted chains and growing chains are identical. Insertions are possible in N-1 different ways, each way having its own probability. These probabilities can be calculated from the 2-dimensional CLD/NBD using the following arguments. The frequency of insertion of a species with a terminal double bond is proportional to its concentration. Therefore, the insertion probability of a polymer chain, containing a certain number of branches, is proportional with this structure's concentration. Consequently, the insertion probability of a polymer chain, containing a certain number of branch points, say N_1, should be proportional with the concentration of chains with N_1 branch points. This probability of insertion of a chain with N_1 is not the only factor playing a role. We additionally need to know the probability of the growing chain, after the first insertion, to obtain precisely that number of branch points to arrive at N branch points in total: $N - N_1 - 1$. Now, during the growth process of a polymer chain, the probability that after the first insertion it will receive this particular additional number of branch points is independent of its growth history. This means that it is independent on whether it grows after the first, second or any insertion and it also is independent on the number of branch points on chains previously inserted. Therefore, the probability that the polymer will grow to obtain the $N - N_1 - 1$ additional branch points is simply proportional to the concentration of such chains. Hence, *under the condition* that a polymer with N branch points is formed, the probability of a first insertion with N_1 branch points equals the normalized product of the concentrations of polymers with a terminal double bond and N_1 branch points and polymers with $N-N_1 - 1$ branch points. For the formation of polymers with a terminal double bond this leads

to the following *conditional* branch point probability density function:

$$\overline{\overline{\Re}}(N_1)\left|\overline{\overline{P}}_N = \frac{\overline{\overline{P}}_{N_1}\overline{\overline{P}}_{N-1-N_1}}{\sum_{j=0}^{N-1}\overline{\overline{P}}_j\overline{\overline{P}}_{N-1-j}} \right. \qquad \text{where } \overline{\overline{P}}_N = \sum_{n=1}^{\infty}\overline{\overline{P}}_{n,N} \tag{1}$$

Note that here $\overline{\overline{P}}_{n,N}$ represents the concentration at the branching catalyst CGC-Ti, $\overline{\overline{P}}^{b}_{n,N}$. The probability density function (pdf) eq 1 expresses the probability of an insertion of a chain with N_1 branch points under the condition that a polymer, with N branch points and a terminal double bond is formed. The pdf $\overline{\overline{\Re}}(N_1)\left|\overline{\overline{P}}_N\right.$ turns out to be a symmetric distribution with high peaks at $N_1 = 0$ and $N_1 = N\text{-}1$ (see Figure 3). This implies that the conditional probability of inserting a chain with zero or N-1 branch points is much higher than that of chains with intermediate number of branch points.

Once the number of branch points on the chain inserted is known, the problem is divided into two smaller sub-problems. The architecture of the inserted chain with N_1 branch points as well as the architecture of the growing chain with $N\text{-}1\text{-}N_1$ branch points must be determined. For both the inserted and the growing chain the same line of reasoning can be used as above for a smaller number of branches, N_1 and $N\text{-}N_1\text{-}1$, respectively. In our algorithm the procedure described above in a recursive manner continues until no more structures with branch points have to be attached.

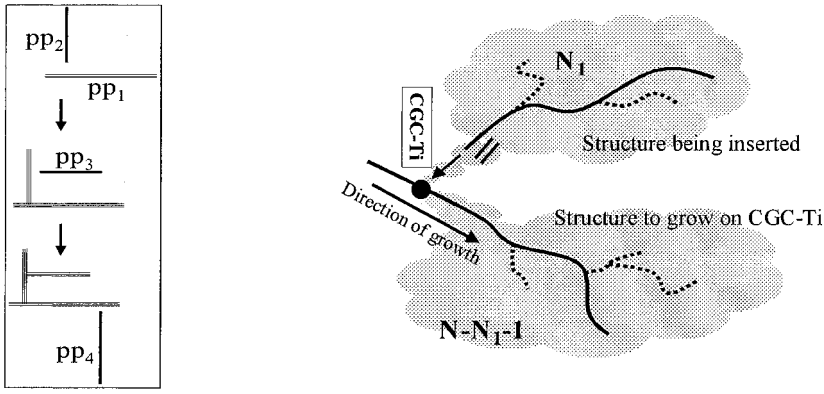

Figure 2 Topology synthesis algorithms for ldPE (left) and metallocene-PE (right).

Then the topology is known. The segment lengths are determined in the same manner as the pp lengths in the ldPE algorithm. The only difference is that this time we need 2N+1 segment lengths, hence the procedure starts by picking 2N numbers.

It is instructive to apply the line of thought after the algorithm to the theoretical extreme that only chains with zero or N-1 branch points are inserted. Then one may easily foresee that a pure *comb* structure will be obtained. We expect that the higher conditional probability of inserting chains with numbers of branch points either close the minimum (0) or the maximum (N-1) will lead to a dominance of comb-like structures. This expectance will be revisited when discussing results.

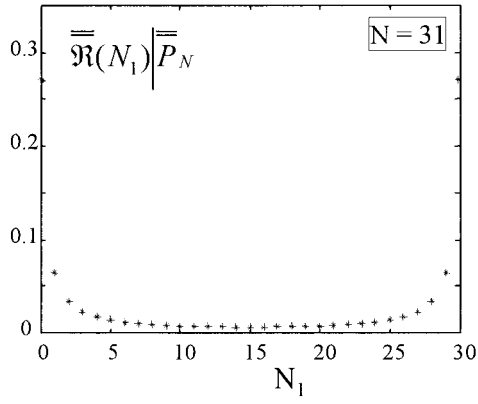

Figure 3
N-pdf according to eq 1 for the case of N = 31 branch points.

Characterization of architectures by radius of gyration

Molecular architectures can be structurally classified as being more comb-like or Cayley tree-like. Structure has impact on the radius of gyration: it is larger for linear molecules than for branched molecules of the same weight (number of monomer units), since the latter are more compact. The ratio between branched and linear radius is usually described by a 'contraction factor'. Furthermore, Cayley tree-like structures are more compact than comb-like structures.[10] We will here show how to obtain the contraction factor from the architectural information. The square radius of gyration $\langle s^2 \rangle$ is expressed in monomeric sizes. According to a statistical-mechanical model[11] it follows from the architecture as represented in graph theoretical terms, the Kirchhoff matrix, **K**, which is derived from the incidence matrix, **C**:[10]

$$\langle s^2 \rangle = n^{-1} Tr(\Lambda_{n-1}^{-1}) \quad (2).$$

Here, n is the number of monomer units and $Tr(\Lambda_{n-1}^{-1})$ denotes the trace of Λ_{n-1}^{-1} being the matrix with n-1 reciprocals of the eigenvalues of the Kirchhoff matrix **K**. The full n x n sized matrix **K** is calculated from:

$$\boldsymbol{K} = \boldsymbol{C}^T \boldsymbol{C} \quad (3),$$

where $\boldsymbol{C}^T$ is the transpose of $\boldsymbol{C}$ (size (n) x (n-1) and γ is a vector of length (n-1) related to the size of monomer units. For the computation of the radius of gyration, we apply a coarse graining method to save on computational effort to find the smallest eigenvalues of **K**.[10] Thus, the Kirchhoff matrix reduces in size, now based on the number of branch points, (2N+2) x (2N+2). In this case the vector γ of length (2N+1) contains the N-1 interbranch segment lengths and the N+2 free arm lengths of the molecule.

We have calculated the radius of gyration distribution for 500 metallocene and ldPE architectures for the case of N = 100 branches and chain length n = 10,000. It should be realized that calculating the radius of gyration requires the full architectural information, including the segment length distribution. The result is shown in Figure 4. We observe that the distribution of metallocene architectures is located at higher contraction factor ranges than the ldPE architectures. This would indicate that the metallocene architectures possess a more comb-like character than the ldPE molecules. This is an interesting result, which never could have been predicted by intuitive means.

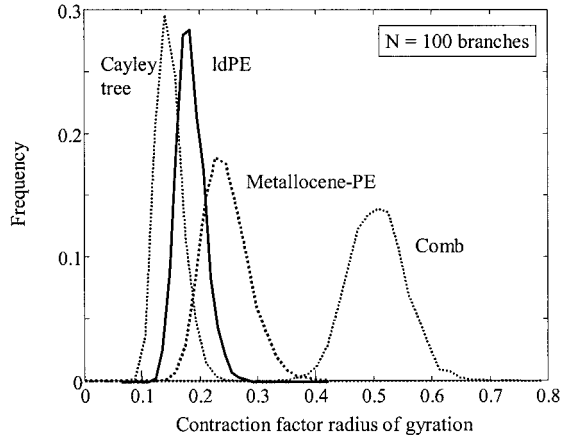

Figure 4
Contraction factor distributions for ldPE and metallocene-PE. Results for extreme Cayley tree and comb topologies also shown.

Rheological qualifiers: seniority and priority.

The concepts of seniority and priority have been introduced[1,12] as ingredients in the application of the "tube" model by de Gennes[12] to hyperbranched polymers. The idea is that reptation, being the typical mode of relaxation for linear polymers, is forbidden for branched polymers, since the chains are no longer free to move along the tube axis due to the presence of branches. This has impact on both the viscous and the elastic behavior of the polymer. Concerning the linear stress relaxation the relaxation time of each segment in the molecules increases with the molecular distance to the nearest free end. It turns out that the linear stress relaxation function completely is determined by the distribution of seniorities. Here, the seniority s_j of a segment j is defined as the molecular distance to the nearest free arm (Figure 2). The seniority of a free arm is one, the value for a segment ending on a terminal branch point is two. Priority is related to elasticity effects occurring during non-linear deformations. The time needed to regain equilibrium is associated with the time required for a deformed chain to retract into its tube. The retraction for a chain segment attached to a number of free ends is hindered, since it is obliged to pull the free ends into its own tube. This is expressed in the priority of that segment and in such a way that branched molecules containing high priority segments feature strong elastic behavior. Priority is defined as follows. Each inner segment is connected to two trees, each of these trees having a number of terminal segments ('free arms'). The priority is the lesser of these numbers of terminal segments.

Computation of bivariate priority and seniority distributions has been done before, for branched metallocene systems.[1] In this case it was possible to find the distributions directly from the kinetic equations, but in general this will not be possible, like in the more complicated ldPE system. Our method of finding the distribution is based on a graph theoretical representation of branched molecules, hence it is independent on specific kinetics. Next we explain briefly how we determine these seniority and priority distributions.

The seniority of a molecular segment between two branch points ('inner' segment) is related to the longest chemical path (LCP) of that segment. In terms of graph theory we say that segments ending on a terminal branch point ('outer' segments) are attached to one and all other segments are attached to two parts of the 'tree' that represents the molecule. The longest chemical path LCP is defined as the highest number of segments in the path to a terminal segment and the inner segments have two of such LCPs: on either side. In a comb most segments have much longer

LCPs than those in a Cayley tree. The seniority of a segment is defined as the lesser of the two LCPs of that segment. The seniority of an outer segment is one, the value for a segment ending on a terminal branch point is two. The priority of a segment is defined as follows. Each inner segment is connected to two trees, each of these trees having a number of terminal segments ('free ends', Figure 5). The priority is the lesser of this number of terminal segments. Priority values are found for each segment (again inner segments only) by constructing balances of terminal segments on either side of the segments.[2]

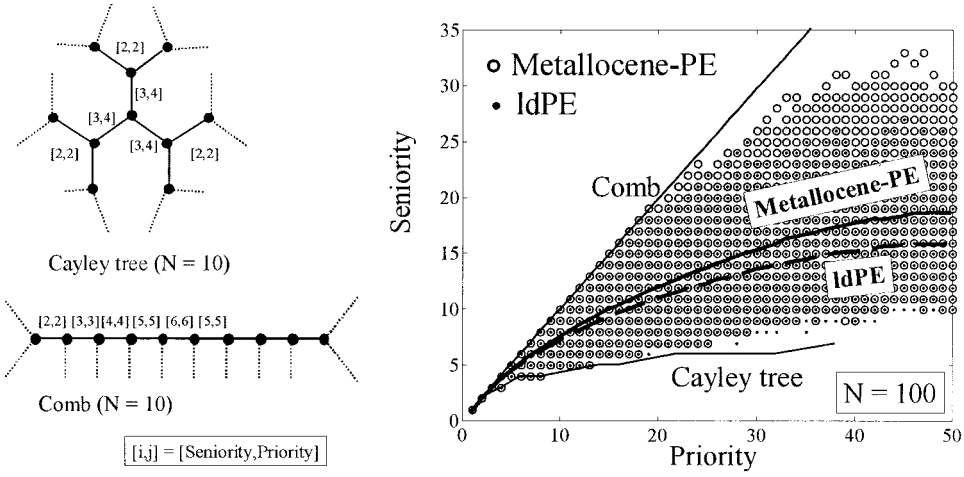

Figure 5
Seniorities and priorities of segments in Cayley tree and comb structure (left). Scatter plot of seniority/priority combinations of segments (right).

Seniorities and priorities have been computed for several ensembles of ldPE and metallocene-PE molecules. In previous work[2] we noticed that plotting seniority values of segments versus priority values provides information on the branching character of branched molecules. When at given priority values seniorities are low, architectures have a Cayley tree-like structure. On the basis of the radius of gyration results we concluded that the metallocene architectures were more comb-like. This then should be in line with the scatter plot of seniorities versus priorities as shown in

Figure 5. This plot contains all the combinations of seniority and priority values found for all the segments of the ensembles of 5000 molecules metallocene PE and ldPE with length 10,000 and 100 branch points. The lower part of the scatter plots of the different products practically overlap, implying that the most star-like structures from both populations are equally star-like. Note from Figure 5 that these most Cayley-like structures still deviate from the theoretical limiting case of a Cayley tree. The upper part of the scatter plot shows that the metallocene structures are more extended into the area of the comb-like structures than the ldPE structures. In addition, one observes that the average seniority versus priority curve for the metallocene system is located at a higher level. We conclude that the seniority/priority results confirm the more comb-like character of the metallocene structures. In addition we observe that the metallocene structures cover a wider range between Cayley tree- and comb-like structures.

Figure 6 shows the bivariate seniority/priority concentration distributions for whole reactor populations of ldPE and metallocene-PE. This in principle represents a full rheological characterization of these systems. Read et al.[1] have computed the full bivariate distribution of seniorities and priorities in an analytical way. The authors generate these for various values of the branching density, b^U in their nomenclature, which is the only adjustable parameter that influences topology. In order to properly make the comparison, we performed simulations at the same values of the branching density, b^U = 0.2, 0.35 and 0.46. Kinetic and reactor data are chosen as before, while catalyst concentrations [Ti-CGC] in the feed of the CSTR to obtain the afore-mentioned branching density values are: [Ti-CGC] = $3.2\ 10^{-7}$, $1.15\ 10^{-6}$ and $6.7\ 10^{-6}$ kmole/m^3, respectively. We have calculated the full bivariate seniority/priority distribution for a reactor population consisting of ensembles of 500 molecules at up to 56 different numbers of branches, at maximum N = 1400. Per ensemble the numbers of segments with identical seniority/priority combination were counted. The noisy shape of the surface at higher seniority/priority is caused by the limited ensemble size (500) and the many combinatorial possibilities of the priority/seniority combinations. Figure 6 can directly be compared to Figure 9 in Read et al.[1], both constructed for b^U = 0.46 or [Ti-CGC] = $6.7\ 10^{-6}$; good agreement is observed. Obviously, the plot obtained by the analytical method does not possess irregular parts, since the problem of ensemble size is irrelevant here. We conclude that in spite of the important differences in the two approaches the agreement is satisfactory.

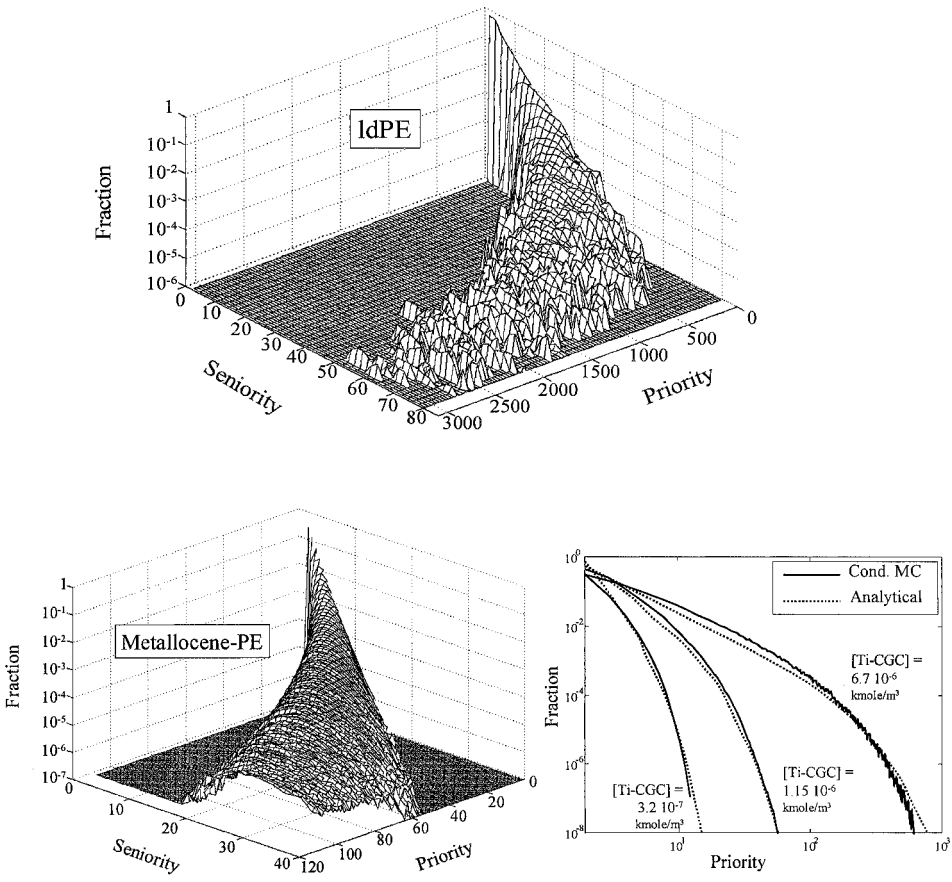

Figure 6
Full reactor populations of seniorities/priorities for ldPE (upper right) and metallocene (lower left). Comparison of priority distributions from analytical solution[1] and conditional MC.

Figure 7 shows the relationship between the lengths of a segment and its priority value for ldPE. This is interesting, since these rheological segment properties are indicative for their location in molecules: in the center or in the periphery. When discussing architectures we already pointed at the impact of the differences in primary polymers residence time distribution on branch point distribution in a molecule. Primary polymers within one molecule that have experienced longer

residence time possess a higher probability of having received branch points. This leads to a heterogeneous structure of molecules, where the primary polymers with the longest residence times are expected to form a centre part with relatively high branching density. These centre parts therefore have shorter average segment lengths, as is confirmed by the figure. The average segment length being 132, the lengths at higher seniority values indeed are much smaller, down to around 50 %.

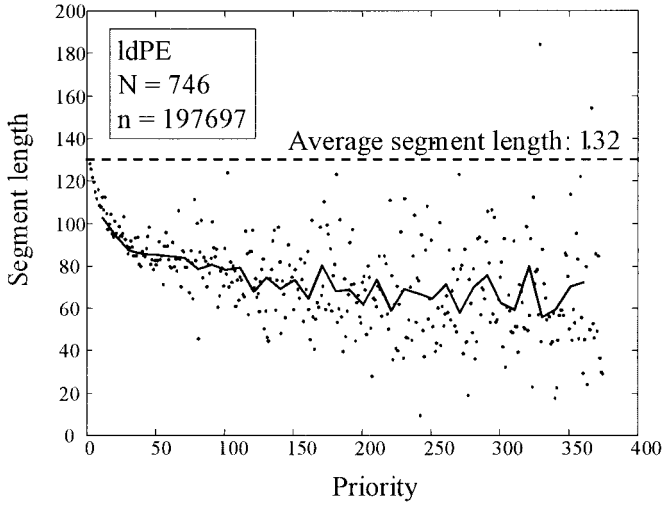

Figure 7
Relation segment length versus priority for ldPE. Dots represent segment length/priority pairs in single molecules, drawn line is the average of all (1000) molecules. At larger priority segment lengths are only 50 % of the average due to heterogeneous branching structure of ldPE.

Conclusion

The architectures generated by our synthesis algorithms revealed marked differences between the two PE-systems. Metallocene-PE turned out to be more comb-like. This can be partially explained by the difference in growth patterns that are simulated by the algorithms. One feature of this is associated to the linear constituting elements, primary polymers for ldPE and segments for metallocene-PE. In both cases these elements all have identical statistics and their length

distribution obeys Flory. In the metallocene system segments are coupled by end points, which in combination with the identical statistics leads to a *homogeneous* branching structure. In contrast, coupling of pps in the ldPE system happens at arbitrary positions along pps. An essential feature of the ldPE synthesis method furthermore is the time sequence of pps within one molecule. This has to be accounted for in view of to the differences in residence time. A pp with longer residence time will on average carry more branch points. This leads to a *heterogeneous* branching structure. Consequently, we found the inner segments (higher priority) to possess the smallest average length. Characterization by radius of gyration and by rheology in terms of priorities and seniorities turned out to be in agreement with each other. They support the main conclusion of this work that the growth pattern in metallocene-PE leads to a more comb-like branching structure than that of ldPE.

[1] D.J. Read, T.C.B. McLeish, *Macromolecules*, **2001**, 34, 1928-1945.
[2] H.C.J. Hoefsloot,, P.D. Iedema, *Macromol. Theory Simul.* **2003**, 12, 484-498.
[3] P.D. Iedema, H.C.J. Hoefsloot, *Macromol. Theory Simul.* **2001**, 10, 855-869.
[4] P.D. Iedema, M. Wulkow H.C.J. Hoefsloot, *Macromolecules,* **2000**, 33, 7173-7184.
[5] P.D. Iedema, S. Grcev, and H.C.J. Hoefsloot, *Macromolecules* **2003**, 36, 458-476.
[6] P.D. Iedema, H.C.J. Hoefsloot, *Macromolecules,* **2003**, 36, 6632-6644.
[7] J.B.P. Soares, A.E. Hamielec, *Macromol. Theory Simul.* **1996,** 5, 547-572.
[8] D. Beigzadeh, D., J.B.P. Soares, T.A. Duever, *Macromol. Rapid Commun.* **1999,** 20, 541-545.
[9] S. Costeux, P. Wood-Adams, D. Beigzadeh, *Macromolecules*, **2002,** 35, 2514-2528
[10] P.D. Iedema, H.C.J. Hoefsloot, *Macromol. Theory Simul.* **2001**, 10, 870-880.
[11] B.E. Eichinger, *Macromolecules* **1980**, 13, 1.
[12] D.K. Bick, T.C.B. McLeish, *Phys. Rev. Letters* **1996**, 76, 14, 2587-2590.